Electronic and geometric structure calculations of adsorption of small $(ZnO)_i$ clusters ($i=1-4$) on graphite

Edward Sanville and Joseph J. BelBruno
Center for Nanomaterials Research and Department of Chemistry, DartmouthCollege, Hanover, New Hampshire 03755, USA
(Received 28 February 2007; revised manuscript received 2 June 2007; published 10 August 2007)

The energetics and configurations of stoichiometric $(ZnO)_i$ clusters on graphite surfaces were investigated using a density functional approach with atomic-type orbitals and relativistic core pseudopotentials. The monomers and dimers were found to take on a vertical arrangement with the zinc atom pointed toward the surface. A cross section of the potential energy surface (PES) was calculated by translation of the cluster across the graphite surface. According to this PES, ZnO and Zn_2O_2 clusters should be free to move about only above a graphitic surface bond at 25 °C. Trimers maintained ring geometries in a parallel orientation to the surface, and the PES suggested that these clusters would most likely be localized with a zinc atom directly above a carbon atom. The tetramers were found to be nearly square and preferentially parallel to the surface. Zn_4O_4, at 25 °C, preferred an orientation with two of the zinc atoms directly above the centers of carbon-carbon bonds. Details of the cluster-graphite bonding interactions were studied using the periodic density functional theory electronic charge densities, analyzed with Bader's atoms in molecules scheme.

DOI: 10.1103/PhysRevB.76.085412 PACS number(s): 36.20.Kd, 36.40.Mr, 71.15.Mb

INTRODUCTION

Cluster deposition on surfaces under a variety of experimental conditions has become an important topic in nanoscience. This interest is driven by the need to understand physical phenomena such as fragmentation,[1] diffusion-limited aggregation,[2–4] and self-assembly[5] of clusters on the substrates. Moreover, the details of adsorbate-surface interactions are essential to the study of nanoelectronic devices. Perhaps the systems most studied are gold or silver atoms and clusters deposited on graphite.[6–12] Graphite is often used as the substrate because of its unique structure as well as its electronic properties. It is characterized by strong sp^2 in-plane bonding and weak coupling between atomic planes, is chemically inert, generally homogeneous, and usually free of defects. Prototypical graphitic studies include the adsorption of carbon materials onto graphite. In particular, the adsorption of fullerene[13] and C_N carbon rings with N ranging from 10 to 16.[14] In recent research efforts, computation and simulation have played a greater role than in previous decades.

Our group has previously explored the structure of gold and silver atoms and clusters on graphite using density functional theory.[15–17] Those results provide some guidance with respect to the current problem. Gold and silver atoms showed little preference for a particular binding site, except that binding over "hollow sites," that is, in the center of a graphite ring, was disfavored. Atomic mobility was determined to be very high. The deformation of graphite surfaces by gold or silver adatoms was small and limited to those adjacent carbon atoms in the top layer. In general, lower layers in the graphite slab were geometrically unaffected by the adatoms, but these lower layers affected the energy landscape. Interestingly, gold dimers were found to preferentially bind in an orientation perpendicular to the surface. Larger gold clusters Au_n ($n=3$, 4, and 5) adopted an orientation, with respect to the graphite, that was cluster dependent.

Semiconductor clusters have attracted considerable research interest. The physical properties of these clusters exhibit size dependence; changes in properties occur as frequently as between neighboring cluster sizes. Matxain *et al.*[18] predicted, via time-dependent density functional theory calculations, a precise pattern of excitation energy changes with cluster size (which involved changes in the overall geometry). Subsequently, Schelly and co-workers[19] reported spectroscopic data that confirmed these predictions. In addition to the practical aspects of such systems, the study of the cluster-surface interface provides an opportunity to explore such interactions on the atomistic scale. Few studies of adsorbed semiconductor clusters are available in the literature. Experimentally, Jing *et al.*[20] have reported a study of Bi_2S_3 on graphite and gold. Computationally, Glaus and co-workers[21] examined the Ag-AgCl interface from a molecular orbital viewpoint. We have recently reported a computational study of small zinc sulfide clusters on graphite. Monomers and dimers were found to prefer vertical surface orientations, while larger clusters were observed to arrange parallel to the surface.[22]

Here, zinc oxide clusters on graphite are explored. Of particular interest is the effect of the substrate on the overall cluster geometry (as compared with the isolated cluster) and the orientation of the cluster on the surface. The electronic properties of the adsorbed cluster are also calculated and compared with those of free clusters.

COMPUTATIONAL METHODS

The software used in this study is the package for linear combination of atomic-type orbitals (PLATO).[23] This package, employing a supercell approach, is especially useful for calculations involving large, periodic systems. It implements a density functional approach with optimized numerical orbitals from both neutral atoms and positively charged ions. Pseudopotentials for the oxygen and carbon cores are adopted from the scheme of Goedecker, Teter, and Hutter,[24] while the pseudopotentials for the zinc cores are taken from those reported by Hartwigsen, Goedecker, and Hutter.[25] The

cutoff radius for numerical integration of overlap integrals was set at 7.0 a.u. from the nucleus of the atoms. The exchange and correlation functionals take the local density approximation (LDA). Extensive, previously reported work with isolated silver and gold clusters[15–17] has shown that the LDA provided more accurate bond lengths and harmonic frequencies for these metal clusters, with respect to experimental values, while systematically overestimating the bond energies. The generalized gradient approximation (GGA) resulted in the opposite behavior. Since our interest here is in the positional bonding and geometry rather than absolute binding energies, we have chosen to continue with the LDA. Valence *s*, *p*, and *d* orbitals optimized from Zn, Zn^+, and Zn^{2+} were used for zinc atoms. The oxygen atom basis set was composed of *s* and *p* valence orbitals optimized from O, O^+, and O^{2+}. The integrals for orbital overlap, kinetic energy, one- and two-center neutral potential terms, nonlocal pseudopotential, and ion-ion interactions are calculated and tabulated prior to use and interpolated during a calculation. The remaining integrals are calculated numerically on an atom-centered mesh. The atom-centered mesh used was composed of 30 radial points, with a maximum integrable angular momentum of 35 a.u., and a maximum angular momentum component of 4 a.u. Multiple Bloch states were included, with eight *k* points for the periodic calculation. Because only periodicity in the *x* and *y* directions was important to the accuracy of the calculations, the grid of Bloch states was limited to the *x*-*y* plane.

Forces are obtained by differentiation of the total energy. The maximum force (in any direction) was converged to within 0.0005 Ry/bohr. Energies converged to within 0.000 01 Ry. These are typical order of magnitude convergence criteria for most computational studies.[17] Partial charges associated with the zinc and oxygen atoms as well as those on nearby carbon atoms on the surface were obtained by standard Mulliken population analysis.

In order to validate the accuracy of PLATO in calculating the geometries of zinc oxide clusters on surfaces, static relaxations were performed on Zn_iO_i clusters in vacuum, without periodic boundary conditions. The PLATO geometries were compared with a set of B3LYP/6-311+G^* full optimizations performed with NWCHEM.[26] Ugalde and co-workers[27] previously reported B3LYP/SKBJ(d) optimization of a similar set of ZnO clusters. Comparison of the PLATO results with both of these DFT calculations shows good agreement, with the largest bond length deviation being 0.02 Å, and the largest bond angle deviation 6.3°.

The application of PLATO to graphite surfaces has been explored previously, where it was shown that the LDA provided a better description of the interlayer energetics and geometry than did the GGA calculations.[15–17] A set of orbitals including neutral atoms and doubly charged ions is sufficient for accurate calculations involving lighter atoms such as carbon. For the Zn_iO_i systems, where $i=1$, 2 or 3, graphite in the supercell was composed of $4\times4\times1$ *AB* unit cells; however, for the Zn_4O_4 system, the supercell surface was composed of a single 6×6 layer. A vacuum layer, half of the unit cell thickness, was left above and below the supercell, in order to isolate the slabs. The carbon atoms composing the top layer of graphite can be classified as either α or β carbon atoms, if they are located directly above a carbon atom in the layer below or above the center of a C_6 ring in the layer below, respectively. Adsorption sites that are located directly above the center of a C_6 ring in the top graphite layer are referred to as hollow sites.

In each full optimization for a cluster on the surface, the cluster was initially placed ~2 Å above the graphite, either perpendicular or parallel to the surface. A zinc atom within the cluster was initially located directly above either an α or a β carbon atom. No constraints were imposed upon the geometric configurations of either the Zn_iO_i clusters, or the underlying graphite substrates.

In addition, for each Zn_iO_i cluster, a series of nine constrained optimizations were performed. The first in each series began with a cluster zinc atom directly above an α carbon in the surface layer of graphite. During the constrained optimization, this zinc atom was allowed to move vertically, away from or toward the graphite surface (the *z* direction), but was not allowed motion in the parallel *x* or *y* directions. The nearest underlying β carbon was also pinned down in all three dimensions. This was done in order to prevent the graphite from moving in the *x* and *y* directions during the optimizations. The remainder of the atoms in the cluster and in the underlying graphite substrate were allowed to move freely in all three dimensions.

The same procedure was repeated, fixing the zinc atom directly above other sites on the graphite surface. These sites included points directly above a β carbon atom, and three points evenly spaced across a surface graphite bond. Optimizations were also performed after fixing the zinc atom directly above a hollow site and three evenly spaced points between the center of the hollow and a β carbon atom within that ring. From the constrained geometry optimizations, an approximation to a cross section of the potential surface was obtained. From this surface, a set of first-order saddle-point geometries were determined, along with the corresponding energy and binding properties.

Bader's atoms in molecules (AIM) approach[23–25] was used to define the bonding interactions between the zinc oxide clusters and graphite. The self-consistent field (SCF) wave functions obtained from the PLATO global minimum geometries were used to calculate ρ, $\nabla\rho$, and $\nabla^2\rho$. Subvolumes that correspond to the topological volume of an atom within the molecule are computed and each volume contains a single atomic nucleus. The presence or absence of a bonding interaction between atomic volumes can be determined by the curvature of ρ at the "critical point" along the shared surface between the atoms where $\nabla\rho=0$. If the critical point corresponds to a first-order saddle point in ρ, a bond exists; otherwise there is no bonding interaction between the two atoms. In order to verify the presence of a bonding interaction between any two atoms in a system, one must therefore find a first-order saddle point $\mathbf{r}_c$ along their shared interatomic surface.

RESULTS AND DISCUSSION

Global minima

We begin by describing the results obtained for unconstrained optimization of the Zn_iO_i clusters on graphite sur-

TABLE I. A comparison of PLATO-optimized Zn_iO_i cluster geometries with a set of B3LYP/6-311+G* full optimizations performed with NWCHEM (Ref. 22) and the calculations of Ref. 27.

	$r_{Zn\text{-}O}$ (Å)			∠ O-Zn-O (deg)		
	Ref. 27	B3LYP/6-311+G*	PLATO	Ref. 27	B3LYP/6-311+G*	PLATO
ZnO	1.713	1.720	1.700			
Zn_2O_2	1.892	1.898	1.886	103.7	102.6	104.1
Zn_3O_3	1.826	1.833	1.818	146.3	144.3	149.5
Zn_4O_4	1.794	1.802	1.784	165.5	163.5	169.4

faces; the determination of the global minimum energy geometries. The starting Zn_iO_i cluster geometries on the surface are those calculated from the PLATO isolated cluster optimizations detailed in Table I. The initial graphite structure is that taken from our previous work.[15–17]

ZnO

For the monomers, three initial orientations relative to the graphite surface were examined. In the first two configurations, the ZnO cluster was located 2.2 Å above the graphite surface, and was oriented perpendicular to the surface, directly above α or β carbon atoms, with the zinc atom pointed toward the surface. In the third orientation, ZnO was placed parallel to the graphite surface, with the zinc atom located 2.2 Å directly above an α carbon atom. Each initial geometry converged to the same final configuration in which ZnO was oriented with its axis perpendicular to the underlying graphite surface, and the zinc atom was nearly above the center of a carbon-carbon bond.

The Zn-O bond length in the final geometry was 1.699 Å, not significantly changed from that in the isolated species, and the zinc atom was positioned 2.063 Å above the plane of the graphite substrate. Mulliken charges on zinc and oxygen were calculated to be $+0.270e$ and $-0.585e$, respectively; in the isolated cluster these charges were $\pm 0.510e$, indicating that the cluster atoms withdrew electron density from the graphite surface, with the majority of the charge density moving onto the zinc atom. The cluster-surface binding energy, defined as $E_{\text{cluster-surface}}-E_{\text{cluster}}-E_{\text{surface}}$, was −1.823 eV. The isolated and bound zinc oxide monomers are shown in Fig. 1. The Mulliken charges on the α and β carbons directly beneath the monomer were −0.065 and −0.069, respectively. The Mulliken charges on the four surrounding carbon atoms were calculated to be in the range +0.033 to +0.035. These values indicate charge transfer to the cluster and the carbons directly beneath the cluster from the surrounding carbon atoms.

Zn_2O_2

The structure of Zn_2O_2 is a diamond-shaped ring of alternating zinc and oxygen atoms. A bonding analysis of the cluster indicates the presence of no bonding interaction between the two zinc atoms. As was true for the monomer, different initial orientations were employed; (1) parallel to the underlying graphite surface, with a zinc atom 2.2 Å above an α carbon atom and (2) perpendicular to the surface, with one of the zinc atoms pointing down and initially 2.2 Å above an α carbon atom. In the latter case, the two oxygen atoms were parallel to the surface. Both initial geometries converged to the same final structure shown in Fig. 1. In the optimized structure, the zinc atom was located 2.117 Å above the plane of the graphite substrate. The zinc atom was located almost exactly above the midpoint of a carbon-carbon bond within the graphite. The Zn-O bonds lengths in the final geometry were 1.901 and 1.863 Å, indicative of a surface influence, because in the isolated species, the bond length was 1.885 Å. The Zn-O bonds closest to the graphite surface were elongated, while those involving zinc farthest from the surface contracted slightly. The O-Zn-O bond angle closest to the graphite surface was 101.7°, while the opposite bond angle was 104.5°; the calculated angle was 104.1° in vacuum. Mulliken charges on the zinc atoms were $+0.536e$ and $+0.654e$, with that closest to the graphite surface more positive. The charge on the oxygen atoms was $-0.745e$. In the isolated cluster, the Mulliken charges were $\pm 0.680e$, indicating that all of the cluster atoms gained electron density. The net Mulliken charge on the cluster adsorbed to the sur-

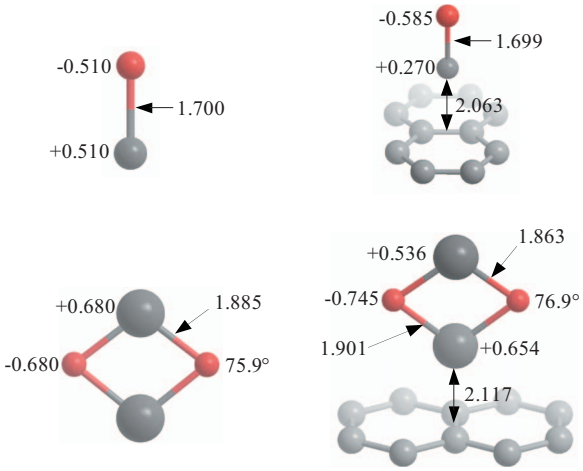

FIG. 1. (Color online) Fully optimized geometries of Zn_iO_i ($i=1,2$), in vacuum (left), and in contact with underlying graphite substrate (right). Bond lengths are given in angstroms, Mulliken charges of symmetry unique atoms are given in units of the elementary charge, and bond angles are given in degrees. The minimum energy orientation for the ZnO cluster (top right) places the bond axis perpendicular to the underlying graphite layer, nearly at the midpoint of two adjacent carbon atoms. The minimum energy orientation for the Zn_2O_2 cluster (bottom right) aligns the zinc-zinc bond axis in a similar position.

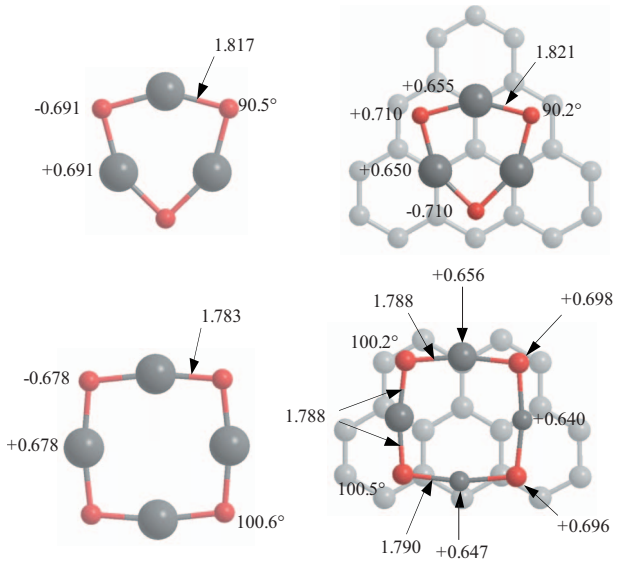

FIG. 2. (Color online) Fully optimized geometries of Zn_iO_i(i =3,4), in vacuum (left), and in contact with underlying graphite substrate (right). Bond lengths are given in angstroms. The minimum energy orientation for the Zn_3O_3 cluster (top right) places the molecular plane parallel to the underlying graphite layer, with the cluster center of mass directly above a graphite α carbon. The minimum energy orientation for the Zn_4O_4 cluster (bottom right) places the molecular plane parallel to the underlying graphite layer, with one zinc atom above a graphite β carbon, and two opposite zinc atoms nearly directly above graphitic carbon-carbon bonds.

face was $-0.300e$ and the cluster-surface binding energy was calculated to be −1.589 eV. The Mulliken charges on the α and β carbons directly beneath the cluster were −0.065 and −0.067, respectively, while the Mulliken charges on the four surrounding carbon atoms were calculated to be in the range +0.022 to +0.025. These charges are very similar to those described in the graphite layer directly beneath the monomer.

Zn_3O_3

In the case of an isolated Zn_3O_3 cluster, the geometry is that of a six-membered, shield-shaped ring of alternating zinc and oxygen atoms. Based on preliminary partial optimizations indicating a preference for a parallel orientation, two initial geometries, both parallel to the surface with (1) a zinc atom directly above either an α carbon atom or (2) a β carbon atom, were fully optimized. The optimized adsorbed cluster is located in a plane parallel to and 2.889 Å above the graphite, as indicated in Fig. 2. The Zn-O bond lengths in the final geometry were all equivalent, 1.821 Å, and essentially identical to the calculated length in the isolated cluster. The O-Zn-O bond angles, 149.8°, and the Zn-O-Zn bond angles, 90.2°, were also unchanged from those in the isolated cluster. Mulliken charges on the zinc atoms were in the range $+0.650e-+0.655e$ and for the oxygen atoms $-0.710e$, while the charges in the isolated cluster were $\pm 0.691e$, indicating withdrawal of charge density from the surface to all of the atoms within the cluster. The net Mulliken charge on the cluster was calculated to be $-0.175e$, and the cluster-surface binding energy was −1.390 eV. The Mulliken charges of the

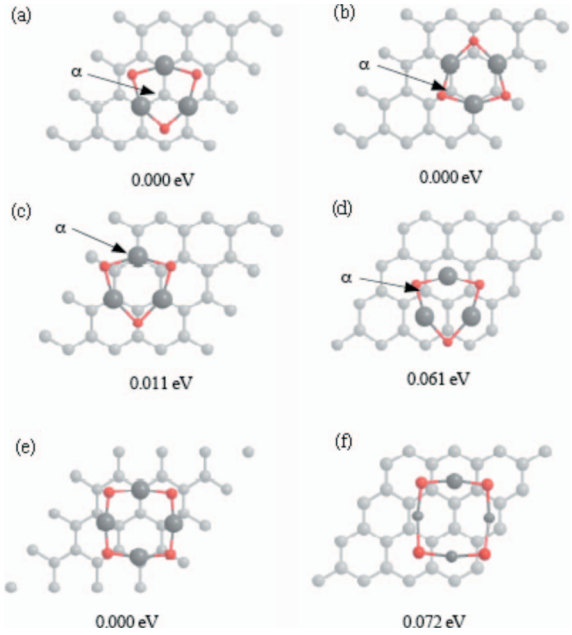

FIG. 3. (Color online) Planar Zn_iO_i clusters on graphite, with binding energies relative to the global maximum given in electron volts: (a) the Zn_3O_3 global maximum binding energy geometry; (b) a related local binding energy maximum; (c) a second and (d) third local binding energy maximum; (e) Zn_4O_4 global maximum binding energy geometry; and (f) local binding energy maximum.

carbon atoms in the top layer of graphite, directly beneath the zinc atoms, were in the range $-0.033e-0.036e$, indicating induced polarization within the underlying graphite sheet. The carbon atoms adjacent to those beneath the zinc atoms had Mulliken charges in the range of $-0.024e$ to $+0.014e$, with the negative atom located beneath the center of the overlying cluster. The Mulliken charges on the carbon atoms nearest the oxygen atoms were in the range of $+0.049e$ to $+0.051e$, while the adjacent atoms had charges in the range of $+0.004e$ to $+0.018e$. These charges indicate that the small net Mulliken charge on the cluster was withdrawn mostly from the carbon atoms nearest to the oxygen atoms.

Three local Zn_3O_3 minima are shown in Figs. 3(b) and 3(d), with their energies relative to the global minimum, Fig. 3(a). An energetic comparison of these four minimum energy structures reveals that the chemical identity of the carbon atoms underlying the zinc atoms determines the relative energies of the structures. Specifically, a binding configuration in which the three zinc atoms are located directly above β carbons is the most stable configuration [see Figs. 3(a) and 3(b)]. In a configuration in which the zinc atoms are directly above α carbons [Fig. 3(c)], the binding energy is destabilized by 0.011 eV relative to the global minimum. Finally, in a configuration in which the three zinc atoms are directly above hollow sites [Fig. 3(d)], the binding energy is destabilized by 0.061 eV relative to the global minimum. It is interesting to notice that the binding sites of the oxygen atoms are relatively unimportant.

Zn_4O_4

The isolated Zn_4O_4 cluster is an eight-membered ring of alternating zinc and oxygen atoms, shaped approximately

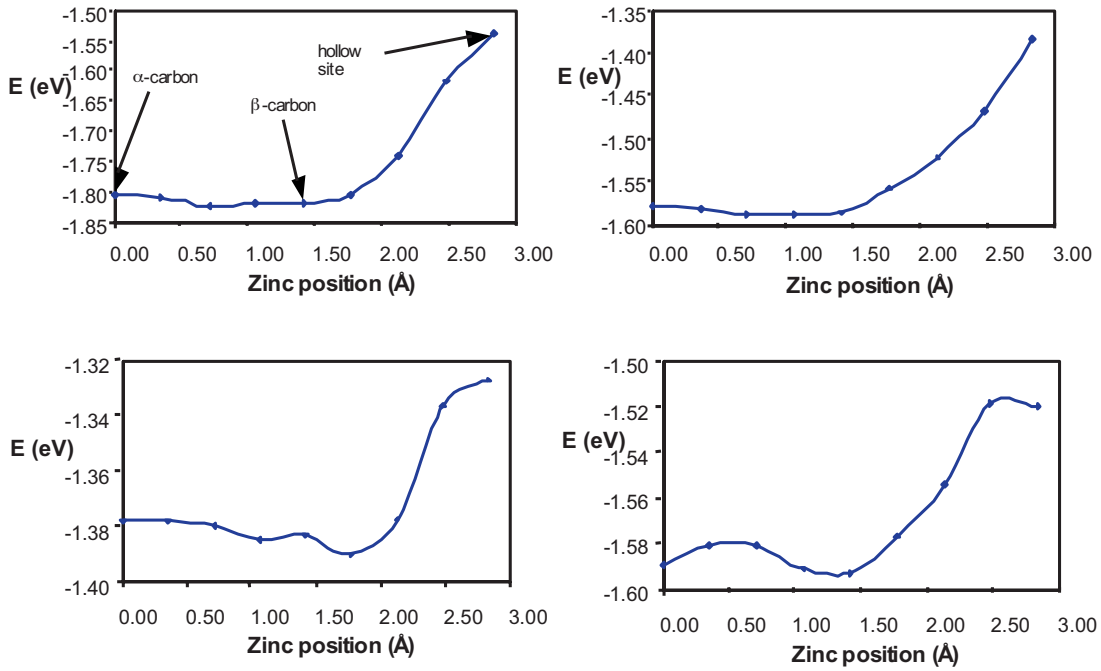

FIG. 4. (Color online) Partial optimization binding energies plotted as a function of the position of the constrained zinc atom above the graphite surface. The x axis represents the horizontal position of the zinc atom from 0.0 Å, (representing a point directly above an α carbon), through 1.414 Å, (representing a point directly above a β carbon), to 2.828 Å (representing a point directly above a hollow site). (a) ZnO on graphite, (b) Zn_2O_2 on graphite, (c) Zn_3O_3 on graphite, and (d) Zn_4O_4 on graphite.

like a square. Three separate full optimizations were performed with different initial geometries: a zinc atom located directly above (1) an α carbon atom, (2) a β carbon atom and (3) a surface hollow. The optimized tetramer cluster structure on graphite, Fig. 2, is oriented with its plane parallel to the surface, at a distance of 2.959 Å. The Zn-O bond lengths in the final geometry averaged 1.789 Å, very slightly elongated from the calculated length in the isolated cluster, 1.783 Å. The overall shape of the cluster distorted from its square initial configuration into a somewhat trapezoidal shape, with C_{2v} symmetry. This shape allowed two opposite zinc atoms to be located almost exactly above the centers of two carbon-carbon bonds on the graphite surface. The Zn-O-Zn bond angles, averaging 100.4°, were not significantly different from the calculated Zn-O-Zn angle of 100.6° within the isolated cluster. Mulliken charges on the zinc atoms were position dependent, but in a very small range ($+0.648e \pm 0.008$), and essentially constant, $-0.697e$, for oxygen. In the isolated cluster the charges were $\pm 0.678e$, indicating that all of the cluster atoms gained electron density upon adsorption to the graphite surface. The net Mulliken charge on the cluster was $-0.206e$ and the cluster-surface binding energy was −1.595 eV. The Mulliken charges on the two carbons forming the bond beneath the two opposite zinc atoms were in the range $-0.014e$–$-0.022e$, while the carbon atom located close to the point beneath the center of the cluster had a Mulliken charge of $-0.011e$. The carbon atoms nearly directly beneath the remaining zinc atoms had Mulliken charges of $-0.033e$, while the carbons closest to the oxygen atoms had Mulliken charges of $+0.049e$. These charges indicate that the small amount of electron density transferred from the surface originated mostly from carbon atoms along the outside of the rings directly beneath the oxygen atoms.

Partial optimizations

The geometric and energetic trends observed across the series of constrained optimizations will be described, as well as the trends in the calculated Mulliken charges on the cluster at every constrained minimum. The adsorption energy for all of the clusters as a function of position on the graphite surface is shown in Fig. 4.

In the final geometry of every partial optimization of the monomer, the molecule was perpendicular to the surface, with the zinc atom lying closest to the graphite. Collectively, the adsorption energies confirm that the lowest-energy position of the zinc oxide monomer is along a surface bond. The lowest-energy *partial optimization* resulted in a geometry in which the fixed zinc atom was directly above the center of the α-β carbon bond. At this point, the adsorption energy is −1.823 eV. However, the binding energy surface is flat along the bond; the energy midway between the carbon atoms is only 0.019 eV less than that obtained when the zinc atom is directly above an α carbon atom, and 0.005 eV less than the energy at the β carbon atom. These energy differences are insignificant. The energy monotonically increases from a β carbon atom to the center of a hollow site, at which point it is 0.287 eV higher than at the center of the carbon-carbon bond. At room temperature, the monomer should have sufficient energy to be completely mobile along the carbon-carbon bond, but is unlikely to be found at a hollow site. As the cluster was translated from above the β carbon atom to a

hollow, its axis tilted slightly so that the β carbon atom remained approximately collinear with the cluster bond axis. At a point halfway between the β carbon and the hollow site, the cluster moved to a position nearly perpendicular to the surface again. The net Mulliken charge tracks the binding energy, reaching a maximum magnitude at $-0.316e$ when the cluster is located in the center of a carbon-carbon bond. This may be due to a large inductive effect as the oxygen atom draws electron density into the cluster. The monomer exhibited the largest net charge of all Zn_iO_i clusters studied. The ZnO-surface distance remains essentially constant with position along the surface, falling in a range of 2.106–2.162 Å. A local minimum in the ZnO-graphite distance was located at the global energy minimum, where the distance was 2.129 Å. The global minimum in the ZnO-graphite distance was found when the zinc atom was located three-fourths of the distance from the β carbon to the position above the surface hollow site, probably as a result of a strained bonding interaction between the zinc atom and the β carbon atom.

The *dimer* prefers a configuration in which the plane of the cluster is perpendicular to the surface, with one zinc atom pointed toward the surface, and the other pointed directly away (see Fig. 1). There is a broad, shallow energy minimum spanning the entire α-β carbon bond. The minimum energy geometry, −1.589 eV, is at a point above the center of the carbon-carbon bond, and 2.129 Å above the plane of the surface. Above the α carbon atom, the binding energy is −1.578 eV, and −1.587 eV above the β carbon atom. The cluster will on average remain above a carbon-carbon bond at 25 °C. It would be unlikely to locate the dimer above a hollow site, since at that point the binding energy decreases to −1.382 eV. The global minimum of $-0.301e$ in the cluster Mulliken charge occurs above the center of the bond. The minimum Zn_2O_2-graphite distance occurs at a point halfway between the β carbon atom and the hollow site, where the distance is 2.129 Å.

The zinc oxide *trimer* relaxed to a configuration in which the plane of the cluster was parallel to the graphite layer; each of the zinc atoms is approximately above a β carbon atom. At this point, the binding energy is −1.390 eV. The binding energy is essentially flat as the selected zinc atom is translated across the carbon-carbon bond (see Fig. 4), and suddenly increases as the cluster moves more than halfway from a β carbon to a hollow site, where the maximum energy, −1.327 eV, is reached. As with the monomer and dimer, this energy difference implies that at 25 °C, the cluster should be relatively free to move such that the zinc atom is located directly above the surface along a carbon-carbon bond. The trimer is the most weakly bound graphite-Zn_iO_i cluster of those studied. The net charge per monomer is consistent with this observation; the magnitude of the maximum charge is only $-0.059e$ per monomer unit, when the zinc atom is directly above the center of a carbon-carbon bond. The charges track the binding energy, reaching a minimum magnitude of $-0.056e$ directly above a hollow site. The trimer Zn-O bond lengths are nearly identical, 1.820 Å, when the zinc atoms are located directly over β carbon atoms. There is some slight cluster distortion as the zinc atoms are positioned between α and β carbon atoms, but this distortion vanishes when all three zinc atoms are above carbon atoms or above hollow sites. The cluster-surface plane distance ranges from 2.785 Å directly above the center of a carbon-carbon bond, to 2.948 Å when a zinc atom is 0.354 Å toward a hollow site from above a β carbon atom.

As with the trimer, the zinc oxide tetramer cluster optimized to a geometry in which the plane of the cluster was parallel to the surface of the graphite. In this geometry, two opposite zinc atoms were located directly above β carbon atoms (see Fig. 2). For each of the constrained optimizations, the cluster was translated so that the zinc atom that was above the β carbon atom in the global minimum geometry was constrained to be directly above an α carbon, a hollow site, or directly above one of seven evenly spaced points in between. The global constrained minimum was the point where the zinc atom was located directly above the β carbon, where the binding energy was −1.593 eV. A local minimum was found where the zinc atom was located directly above the α carbon, at which the binding energy was −1.589 eV, and a second local minimum was found where the zinc atom was located above a hollow site, where the binding energy was −1.519 eV. The binding energy as a function of position is shown in Fig. 4(d). The cluster Mulliken charges per monomer unit track the binding energy, and were very small at every point studied, approximately equal to those of Zn_3O_3. The cluster charge magnitude (per monomer unit) reached a maximum when the zinc atom was directly above a bond, where it was $-0.055e$, and a minimum when the zinc atom was directly above a hollow site, where it was $-0.049e$. The cluster geometry distorts only very slightly at the points studied, with typical bond lengths within the cluster ranging between 1.786 and 1.791 Å. When the tetramer is located with the zinc atom directly above a hollow site, the cluster-surface distance is at its maximum of 3.012 Å. The cluster-surface distance reaches a global minimum of 2.904 Å when the fixed zinc atom is approximately one-fourth of the way from the α carbon along the carbon-carbon bond and a local minimum, 2.960 Å, when the fixed zinc is halfway from a β carbon to a hollow site.

At this point a comparison with the previously reported zinc sulfide clusters is appropriate. In general, the relative orientations, perpendicular vs parallel, are identical for the two sets of clusters. However, all of the zinc oxide adsorbates lie closer to the surface and, hence, experience greater adsorption energy. This may be a reflection of the greater polarity within the oxide molecules. There are some specific differences between particular members of the two sets of clusters. The zinc oxide trimer adsorption is strongest when the zinc atoms are located over β carbon atoms; the small difference between that position on the surface and a translated position in which the zinc atoms are over α carbon atoms, indicates approximately equal stability on the surface. There is a small, but distinct, barrier for such movement along the surface for the zinc sulfide trimer. Zn_4S_4 is situated with two zinc atoms directly over -C-C- bonds and two others over hollow sites. The analogous Zn_4O_4 cluster is distorted from its isolated square geometry and has two zinc atoms approximately over α carbon atoms and the two other zinc atoms over -C-C- bonds. The differences between the energetics for Zn_4O_4 and Zn_4S_4 can probably be understood in terms of geometry. The zinc oxide tetramer is slightly

TABLE II. Zn_iO_i AIM data. Bonded atoms, electronic charge density Hessian eigenvalues λ_1, λ_2, and λ_3, the Laplacian at the bond critical point, and the calculated bond strain angle for all detected cluster-surface interactions analyzed with Bader's atoms in molecules approach. Only symmetry-unique bonds are shown for Zn_4O_4.

System	Atom *A*	Atom *B*	λ_1	λ_2	λ_3	$\nabla^2\rho(\mathbf{r}_c)$	Bond strain angle (deg)
ZnO	Zn	α C	−0.0600	−0.0106	0.2191	0.1485	20.17
Zn_2O_2	Zn	β C	−0.0534	−0.0071	0.1984	0.1379	42.69
Zn_3O_3	Zn-1	C-24	−0.0077	−0.0072	0.0513	0.0364	2.51
	Zn-3	C-20	−0.0076	−0.0063	0.0489	0.0350	1.88
	O-2	C-40	−0.0054	−0.0017	0.0387	0.0316	12.53
	O-4	C-8	−0.0054	−0.0016	0.0386	0.0315	12.86
	Zn-5	C-36	−0.0076	−0.0063	0.0489	0.0350	1.88
Zn_4O_4	Zn-1	C-9	−0.0066	−0.0059	0.0447	0.0321	2.77
	O-2	C-10	−0.0053	−0.0016	0.0378	0.0309	11.78
	Zn-3	C-11	−0.0074	−0.0023	0.0409	0.0312	18.37
	O-4	C-12	−0.0042	−0.0023	0.0416	0.0352	3.89
	Zn-5	C-13	−0.0075	−0.0049	0.0446	0.0322	4.11
	O-6	C-14	−0.0043	−0.0015	0.0403	0.0345	4.09
	Zn-7	C-15	−0.0075	−0.0023	0.0415	0.0317	22.63
	O-8	C-16	−0.0053	−0.0016	0.0385	0.0315	12.22
Graphite Interlayer	C	C	−0.0020	−0.0019	0.0247	0.0208	0.46

smaller in diameter, with slightly more acute chalcogenide-Zn-chalcogenide angles than in the zinc sulfide tetramer. As a result, it is not geometrically possible to achieve the alignment present in the global minimum zinc sulfide cluster, in which two opposing zinc atoms are directly above the centers of carbon-carbon bonds such that the bonds run parallel to the chalcogenide-zinc-chalcogenide bond in the cluster. In general, it can be expected that clusters of even slightly different sizes and geometries will demonstrate markedly different potential energies along the surface of a periodic substrate such as graphite, despite their similar overall chemistry.

Bader analysis

The cluster-graphite bonding interactions were further studied using Bader's atoms in molecules analysis.[28–30] The critical points $\mathbf{r}_c$ on $\rho(\mathbf{r})$ were located and characterized. The Hessian matrix was then calculated and diagonalized for each critical point. Critical points with exactly two negative and one positive Hessian eigenvalue (see Table II), are considered first-order saddle points, or $(3,-1)$ critical points. Within the structure of AIM theory, these critical points indicate the presence of a bonding interaction between adjacent atomic volumes. Additionally, bonds can be classified as either closed shell or shared electron (covalent) interactions, if the Laplacian of the electron density is positive or negative at the bond critical point, respectively. A bond strain angle can be calculated as the angular deviation of the nucleus-$\mathbf{r}_c$-nucleus angle from 180°.

In the ZnO monomer case, the Bader analysis revealed that there was a strong, closed-shell interaction between the cluster zinc atom and the underlying carbon atom within the top layer of the graphite substrate. The zinc atom is bound to the β carbon (see Fig. 5), with a relatively large bond strain angle of 20.17°, probably due to the close proximity of the zinc atom to the area above the center of the surface carbon-

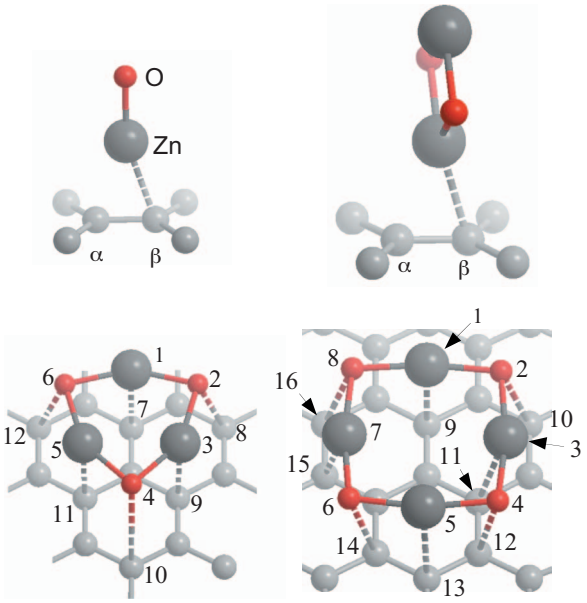

FIG. 5. (Color online) Cluster-surface bonding obtained via AIM theory. Top left: ZnO. Top right: Zn_2O_2. Bottom left: Zn_3O_3. Bottom right: Zn_4O_4.

carbon bond. In fact, the position of this bond critical point is also shifted, from the axis directly between the zinc and carbon atoms, toward the center of the graphitic carbon-carbon bond. The adsorption point is assigned to the β carbon, because according to AIM methodology, tracing the gradient uphill in energy from the bond critical point along both directions of the Hessian eigenvector with the positive eigenvalue, locates a point above the two nuclei associated with that particular bond. Such a procedure links the zinc atom with a β carbon atom, rather than an α carbon atom (or both atoms, as might be expected for a delocalized bond).

The zinc oxide dimer was located directly above the center of a carbon-carbon bond at its global minimum configuration. The Bader analysis indicates that the zinc atom is bound to the β carbon atom within the carbon-carbon bond, with a substantial bond strain angle of 42.69°. Within the clusters themselves, no Zn-Zn bonding interaction was discovered. This is consistent with the long Zn-Zn distance in the zinc oxide dimer.

In the case of trimers, bond critical points were located between each of the six atoms within the zinc oxide clusters, and the underlying carbon atoms. The zinc oxide tetramer contained eight bonds to the graphite surface, involving every atom within the cluster. For both the trimer and tetramer, the Hessian eigenvalues for each critical point were an order of magnitude smaller than the corresponding eigenvalues in the case of the monomer and dimer bonds, indicating the presence of a different type of bonding. The magnitudes of the eigenvalues of the Hessian matrix for these two adsorbates are found to correspond well to the eigenvalues present at the critical points in interlayer graphite π-stacking interactions (Table II). This, combined with the similarity of the cluster-surface distance with the graphitic interlayer distance, is interpreted as evidence that the binding in the trimer- and tetramer-graphite interactions is of the same magnitude as a "π-π"-like orbital interaction. The present calculations do not allow for an unambiguous assignment as such. In all cases, the Laplacian of the electronic charge density at the bond critical point was positive, indicating a closed-shell interaction between the cluster and the surface.

CONCLUSIONS

It was determined that strong, noncovalent bonds are formed between the zinc atom in a monomer or dimer and graphite. The minimum energy configuration for both of these small clusters is such that the cluster is oriented perpendicular to the graphite surface. Additionally, they are predicted to be free to move along the carbon-carbon bonds at 25 °C. The AIM bonding analysis revealed that the only cluster-surface bond was formed between the zinc atom and the β carbon. The trimer and tetramer were found to prefer orientations parallel to the graphite surface; the trimer with an orientation in which all three of its zinc atoms were directly above the β carbon atoms and the tetramer with two of its zinc atoms were directly above carbon-carbon bonds two other zinc atoms directly above carbon atoms. Weak π-stacking interactions were observed between both the trimer and tetramer, and the underlying graphitic surfaces. Marked differences between Zn_iS_i and Zn_iO_i adsorption were hypothesized to be geometric in origin.

ACKNOWLEDGMENTS

The authors gratefully acknowledge S. D. Kenny and A. P. Horsfield for their efforts in developing the PLATO software and for allowing us to participate in its distribution.

[1] Y. Tai, W. Yamaguchi, Y. Maruyama, K. Yoshimura, and J. Murakami, J. Chem. Phys. **113**, 3808 (2000).
[2] P. J. Feibelman, Phys. Rev. Lett. **58**, 2766 (1987).
[3] I. M. Goldby, L. Kuipers, B. von Issendorff, and R. E. Palmer, Appl. Phys. Lett. **69**, 2819 (1996).
[4] M.-H. Schaffnery, J.-F. Jeanneret, F. Patthey, and W.-D. Schneider, J. Phys. D **31**, 3177 (1998).
[5] L. Motte, E. Lacaze, M. Maillard, and M. P. Pileni, Langmuir **16**, 3803 (2000).
[6] S. J. Carroll, S. Pratontep, M. Streun, R. E. Palmera, S. Hobday, and R. Smith, J. Chem. Phys. **113**, 7723 (2000).
[7] W. Yamaguchi, K. Yoshimura, Y. Tai, Y. Maruyama, K. Igarashi, S. Tanemura, and J. Murakamia, J. Chem. Phys. **112**, 9961 (2000).
[8] D. J. Kenny, R. E. Palmer, C. F. Sanz-Navarro, and R. Smith, J. Phys.: Condens. Matter **14**, L185 (2002).
[9] N. R. Gall, E. V. Rut'kov, and A. Y. Tontegode, JETP Lett. **75**, 26 (2002).
[10] A. Courty, I. Lisiecki, and M. P. Pilenia, J. Chem. Phys. **116**, 8074 (2002).
[11] E. Ganz, K. Sattler, and J. Clarke, Phys. Rev. Lett. **60**, 1856 (1988).
[12] E. Ganz, K. Sattler, and J. Clarke, Surf. Sci. **219**, 33 (1989).
[13] R. S. Ruoff and A. P. Hickman, J. Phys. Chem. **97**, 2494 (1993).
[14] J. M. Ugalde, J. Phys. Chem. B **106**, 6871 (2002).
[15] G. M. Wang, J. J. BelBruno, S. D. Kenny, and R. Smith, Surf. Sci. **541**, 91 (2003).
[16] G. M. Wang, J. J. BelBruno, S. D. Kenny, and R. Smith, Phys. Rev. B **69**, 195412 (2004).
[17] G. M. Wang, J. J. BelBruno, S. D. Kenny, and R. Smith, Surf. Sci. **576**, 107 (2005).
[18] J. M. Matxain, J. M. Mercero, J. E. Fowler, and J. M. Ugalde, J. Am. Chem. Soc. **125**, 9494 (2003).
[19] S. Wu, N. Yuan, H. Xu, X. Wang, and Z. A. Schelly, Nanotechnology **17**, 4713 (2006).
[20] T. W. Jing, N. P. Ong, and C. J. Sandroff, Appl. Phys. Lett. **53**, 104 (1988).
[21] S. Glaus, G. Calzaferri, and R. Hoffmann, Chem.-Eur. J. **8**, 1786 (2002).
[22] E. Sanville and J. J. BelBruno, Phys. Rev. B **73**, 085416 (2006).
[23] S. D. Kenny, A. P. Horsfield, and H. Fujitani, Phys. Rev. B **62**, 4899 (2000).
[24] S. Goedecker, M. Teter, and J. Hutter, Phys. Rev. B **54**, 1703 (1996).

[25] C. Hartwigsen, S. Goedecker, and J. Hutter, Phys. Rev. B **58**, 3641 (1998).
[26] T. P. Straatsma *et al.*, Computer code NWChem 4.5 (Pacific Northwest National Laboratory, Richland, WA 99352, 2003).
[27] J. M. Matxain, J. E. Fowler, and J. M. Ugalde, Phys. Rev. A **62**, 053201 (2000).
[28] R. F. W. Bader, *Handbook of Molecular Physics and Quantum Chemistry* (John Wiley and Sons, Chichester, UK, 2003), Vol. 2.
[29] R. F. W. Bader, *Atoms in Molecules: A Quantum Theory* (Oxford University Press, Oxford, 1990).
[30] R. F. W. Bader, http://www.chemistry.mcmaster.ca/aimpac/